

MAY 1980

LRP 167/80

NONLINEAR-MODULATION OF ION BEAM MODE

T. Honzawa⁺ and Ch. Hollenstein

⁺ Present address: Department
of Electronic Engineering,
Utsunomiya University,
Utsunomiya 321-31, Japan

NONLINEAR SELF-MODULATION OF ION BEAM MODE

T. Honzawa⁺ and Ch. Hollenstein

+ Present address: Department
of Electronic Engineering,
Utsunomiya University,
Utsunomiya 321-31, Japan

Abstract

Nonlinear self-modulation of the fast ion beam mode is experimentally studied. At large amplitudes above threshold the beam mode is observed to be amplitude-modulated by the self-action. The instability appearing on the carrier wave envelope is found to rapidly grow with increasing distance and then be saturated. When the self-modulation deeply proceeds, the wave envelope splits into a train of wave packets. Finally we show that the self-modulation can be explained to come from the modulational instability.

Evolution of wave envelopes due to nonlinear effects is an attractive subject of plasma physics. A number of theoretical works¹ on the nonlinear evolution of plasma wave envelope have been reported so far. Kakutani and Sugimoto² and Chan and Seshadri³ have indicated that the ion plasma mode becomes modulationally unstable only for large wavenumbers $k > k_c$, at which ion Landau damping is usually very strong. On the other hand, Ikezi et al.⁴ have shown, both experimentally and by computer simulations, that for the ion acoustic wave the ions trapped in the wave potential troughs introduce effects so much larger than the modulational instability that the ion acoustic wave can not be modulationally unstable. On the contrary Watanabe⁵ has postulated on the basis of his experiment that the ion acoustic wave can become modulationally unstable. However, it seems that his experimental data⁵ demonstrate essentially the same properties of the ion acoustic wave packets as those observed by Ikezi et al.⁴, that is, the data show that the wave packets do not shrink but expand during wave propagation. In this paper, we wish to report experimental results on the self-modulation of the fast ion beam mode and show that this self-modulation can be explained to come from the modulational instability.

Experiments were carried out using a double plasma device⁶ containing plasmas with densities $N_e \sim 10^9 \text{ cm}^{-3}$, electron temperature $T_e \sim 1 \text{ eV}$ and ion temperature $T_i \sim 0.2 \text{ eV}$. Application of a potential ϕ to the "driver" plasma caused an ion beam into the "target" plasma. Here, an ion beam with velocity $v_b \sim C_s$, where C_s is the ion acoustic velocity, was used. In order to excite waves in the ion beam-plasma system, the potential ϕ was externally modulated at a frequency $\omega_o \approx (0.4 \sim 0.5)\omega_{pi}$, where

$\omega_{pi}/2\pi \approx 1.4$ MHz. In this case the excited wave was a plane wave because of the large diameter of the separating grid. Further, although the effective temperature and average velocity of the beam ions were a little increased by the external modulation of ϕ , observations showed that the increase in phase velocity of the excited wave was below a few % of the initial one, even if the rf (peak-to-peak) voltage V_{pp} externally applied was as high as 3 V. A Langmuir probe and an ion energy analyzer were used for measurements of plasma parameters and excited waves. Wave patterns were measured by means of an interferometric technique using a cross correlator⁷. A frequency analyzer was also used to observe frequency spectra.

At small rf voltage V_{pp} only a wave could be observed at far distance x from the excitation plane. Dispersion relation of linear waves excited in the system is given in Fig.1 together with those for waves computed on the basis of a linear theory⁸. Comparison of the experimental result with the theoretical one leads us to conclude that the observed wave belongs to the *fast* ion beam mode. Figure 1 also gives the dispersive phase velocity v_p and group velocity v_g of the fast ion beam mode computed for the same condition.

When V_{pp} was increased, the wavenumber of the beam mode was observed to decrease from the linear value especially around the first minimum of the wave amplitude, as shown in Fig.2. The maximum wavenumber shift was found to increase with increasing V_{pp} . Details of the experiment on the nonlinear wavenumber shift will be described elsewhere. Further, at large V_{pp} above threshold the carrier wave at ω_0 was observed to be amplitude-modulated. Figure 3 demonstrates the occurrence of the amplitude-modulation

at large amplitudes above threshold. We can also see from this figure that the instability appearing on the wave envelope rapidly grows with increasing x and is saturated at some distance. Here, it should be noted that at a suitable value of V_{pp} the wave envelope is scarcely modulated at small x , even if the violent modulation is observed at large x . This tells us that the amplitude-modulation of the carrier wave is caused not by some external source but by the nonlinearity of the wave itself. Moreover, at large V_{pp} above threshold a low frequency peak was observed to appear together with two sideband peaks near the main peak at ω_0 in a spectrum as shown in Fig.4. From such spectra we can know the V_{pp} -dependence of wave amplitude corresponding to each peak as well as the one of the carrier amplitude, as illustrated in Fig.5. The spatial variation of wave amplitudes is also obtained as given in Fig.6. On the other hand, when the self-modulation deeply proceeds, the wave envelope is observed to split into a train of wave packets (see Fig.7). For each wave packet we could find the change of the local carrier frequency. Figure 8 indicates statistically the existence of a difference in the local carrier frequency between upstream and downstream.

It is known from observations of the nonlinear wavenumber shift that the phase velocity v_p of the fast ion beam mode increases with increasing amplitude. Therefore, we can say that the phase at point B moves faster than those at points A and C in Fig.9. As a result the wave pattern between A and B is compressed and hence the frequencies over there become a little higher than the initial one, whereas the wave pattern between B and C is stretched and the frequencies become lower. This phenomenon is actually observed (see Fig.8). After the frequency

modulation considerably proceeds, the part of the wave between B and C has a faster group velocity than that of the part between A and B because of the dispersive property of v_g (see Fig.1). This means that the wave is modulationally unstable.

Next, let us consider the self-modulation on the basis of existing theory. Writing the amplitude of the carrier wave with linear frequency ω_0 and wavenumber k_0 in a form such as

$$a = \frac{\delta N}{N_0} = \psi(x, t) \exp[i(k_0 x - \omega_0 t)], \quad (1)$$

the evolution of the wave envelope can be expressed by means of the nonlinear Schrödinger equation as⁹

$$i \frac{\partial \psi}{\partial \tau} + p \frac{\partial^2 \psi}{\partial \xi^2} + q |\psi|^2 \psi = 0, \quad (2)$$

where new coordinates such as

$$\xi = x - v_g t \quad \text{and} \quad \tau = t, \quad (3)$$

are used. The coefficients $p = (1/2) (\partial^2 \omega / \partial k^2)_0$ and $q = -(\partial \omega / \partial |\psi|^2)_0$ and the group velocity v_g are the values evaluated at $\psi = 0$.

Introducing two real variables ρ and σ such as

$$\psi = \rho^{1/2} \exp(i \int \sigma d\xi / 2p) \quad (4)$$

and substituting this expression into eq.(2), we have a pair of equations for ρ and σ as

$$\frac{\partial \rho}{\partial \tau} + \frac{\partial (\rho \sigma)}{\partial \xi} = 0, \quad (5a)$$

and

$$\frac{\partial \sigma}{\partial \tau} + \sigma \frac{\partial \sigma}{\partial \xi} = 2pq \frac{\partial \rho}{\partial \xi} + p^2 \frac{\partial}{\partial \xi} \left[\rho^{-1/2} \frac{\partial}{\partial \xi} \left(\rho^{-1/2} \frac{\partial \rho}{\partial \xi} \right) \right]. \quad (5b)$$

Here, if we write the variables ρ and σ in forms such as

$$\rho = \rho_0 + \delta \rho \exp[i(K\xi - \Omega\tau)] \quad (6a)$$

$$\sigma = \sigma_0 + \delta \sigma \exp[i(K\xi - \Omega\tau)] \quad (6b)$$

and substitute these into the linearized equations of (5a) and (5b), the dispersion relation for K and Ω as follows,

$$\Omega = K\sigma_0 + (-2pq\rho_0)^{1/2}K + O(K^3), \quad (7)$$

is obtained, provided that ρ_0 is finite. Eq.(7) indicates that the wave envelope can be modulationally unstable for small K if $pq > 0$. Applying this theory to our experiment, we can show $p < 0$ from Fig.1 and $q < 0$ from observed nonlinear wavenumber shifts and hence $pq > 0$.

In the case that $pq > 0$, the growth rate of the modulational instability is given from eq.(7) as

$$\gamma = (2pq\rho_0)^{1/2}K, \quad (8)$$

which is proportional to K and $\rho_0^{1/2}$ ($= \psi_0$), where ψ_0 is the initial carrier amplitude. Further, under the same condition eq.(2) gives a solitary wave solution, which tends to zero for $|\xi| \rightarrow \infty$. This solution is of the form as⁹

$$\psi = \psi_s \operatorname{sech}[(q/2p)^{1/2}\psi_s \xi] \exp[i(q\psi_s^2/2)\tau]. \quad (9)$$

Hence, the width of this solitary wave $\Delta\xi$ is such as

$$\Delta\xi \approx 2.6(2p/q)^{1/2}/\psi_s, \quad (10)$$

which is inversely proportional to its amplitude ψ_s like a usual solitary wave¹⁰. However, the velocity of the solitary wave does not depend on ψ_s and is equal to the group velocity v_g . Applying eq.(10) to our experiment, the width $\Delta\xi$ is estimated to be $\Delta\xi \sim 2$ cm, which is several times larger than the carrier wave wavelength ($\lambda_0 \approx 0.4$ cm). Further, assuming $K \approx 2\pi/(2\Delta\xi)$, we can estimate the average frequency corresponding to these solitary signals as $\Delta\omega/2\pi \approx v_g/(2\Delta\xi) \sim 60$ kHz. This is very close to the average frequency of the low frequency peak observed in spectra (see Fig.4). Using eq.(8), we can also estimate the growth rate as $\gamma \sim 10^5 \text{ sec}^{-1}$, which is close to the observed value ($\gamma_{ob} \approx v_g/L \sim 2 \times 10^5 \text{ sec}^{-1}$, where L is the growth length). From these results we conclude that the solitary signals on the carrier wave

envelope, corresponding to the low frequency peak in spectra, are generated by the modulational instability. On the other hand, the upper and lower sideband peaks near the main peak at ω_0 can be considered to result from the nonlinear mode coupling between the carrier wave and low frequency wave thus generated.

In conclusion, we have described experiments on the self-modulation of the fast ion beam mode. The experiments show that in an ion beam-plasma system with beam velocity $v_b \sim C_s$ only the beam mode is observed at far distances from the excitation plane and its nonlinear properties are well studied. Further, at large amplitudes the amplitude-modulation of the beam mode, being a carrier wave, as well as the nonlinear wavenumber shift is observed to be induced by nonlinear effects. As a result of the amplitude-modulation the carrier wave envelope splits into a train of wave packets. Such observational results including the ones obtained from spectral analysis are well explained by existing theory on the modulational instability.

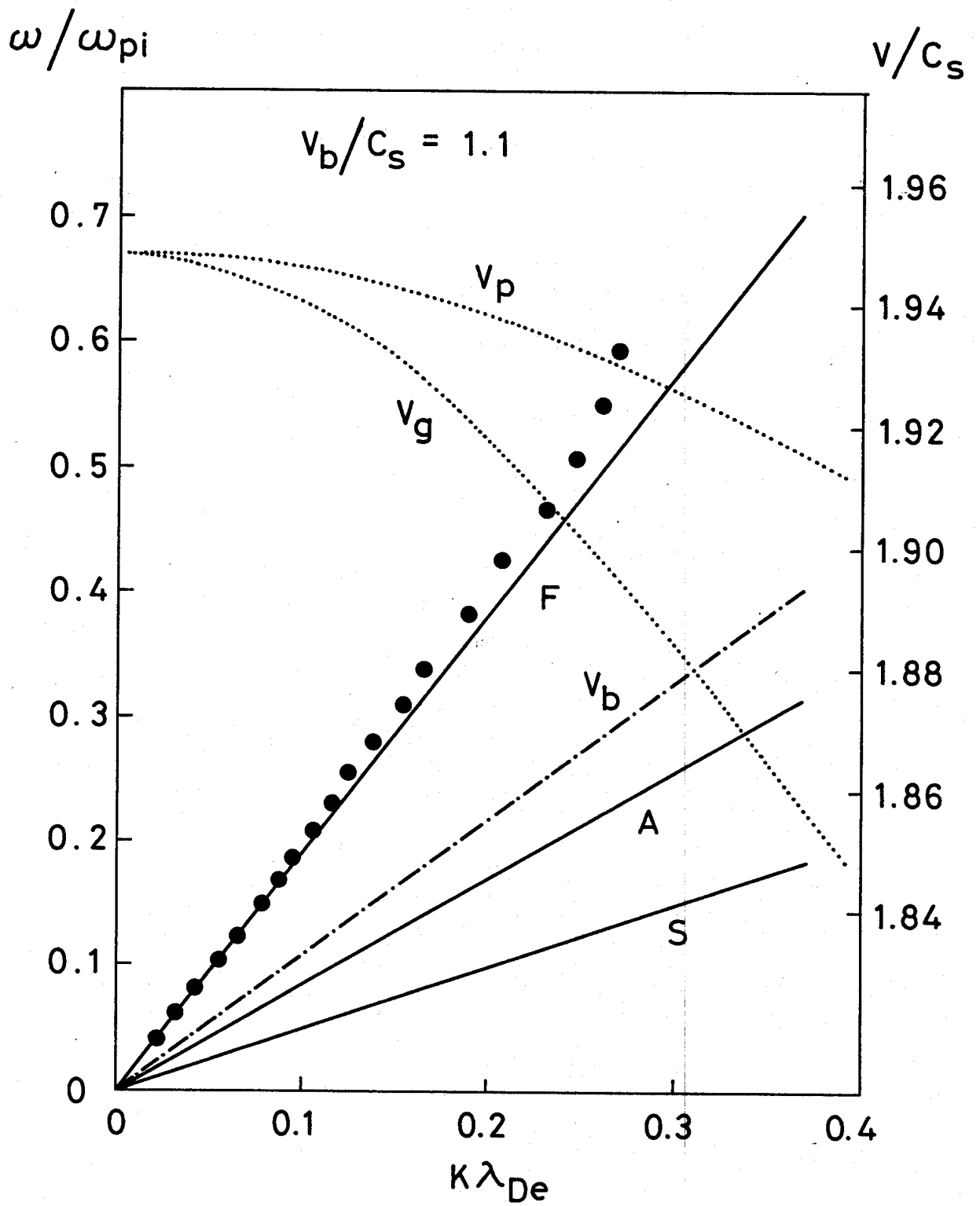
We thank Prof. K. Matsuura, Dr. J. Vaclavik and Dr. R. Bingham for valuable discussions, Mr. P. J. Paris and Mr. M. Guyot for technical supports and Mr. Y. Sumiyoshi for computations. We are also grateful to Prof. E. S. Weibel for encouragement.

References

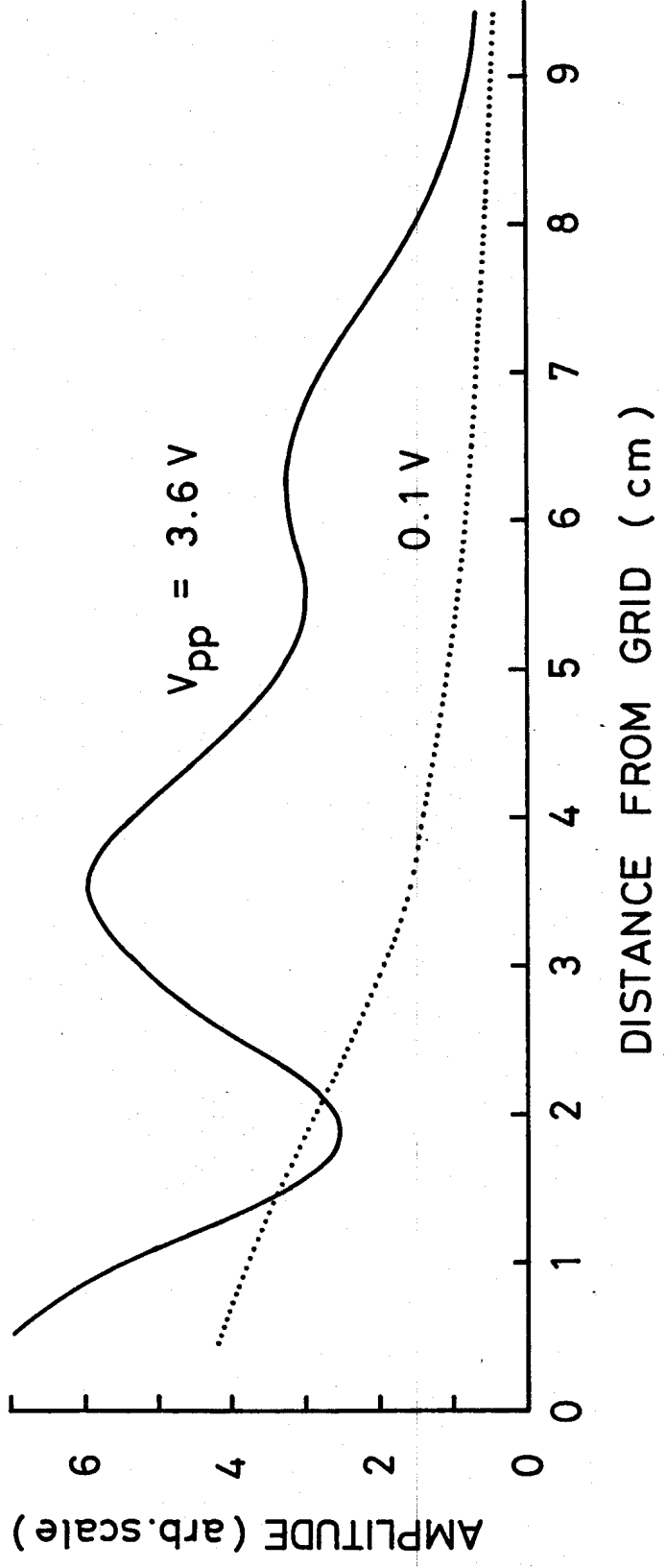
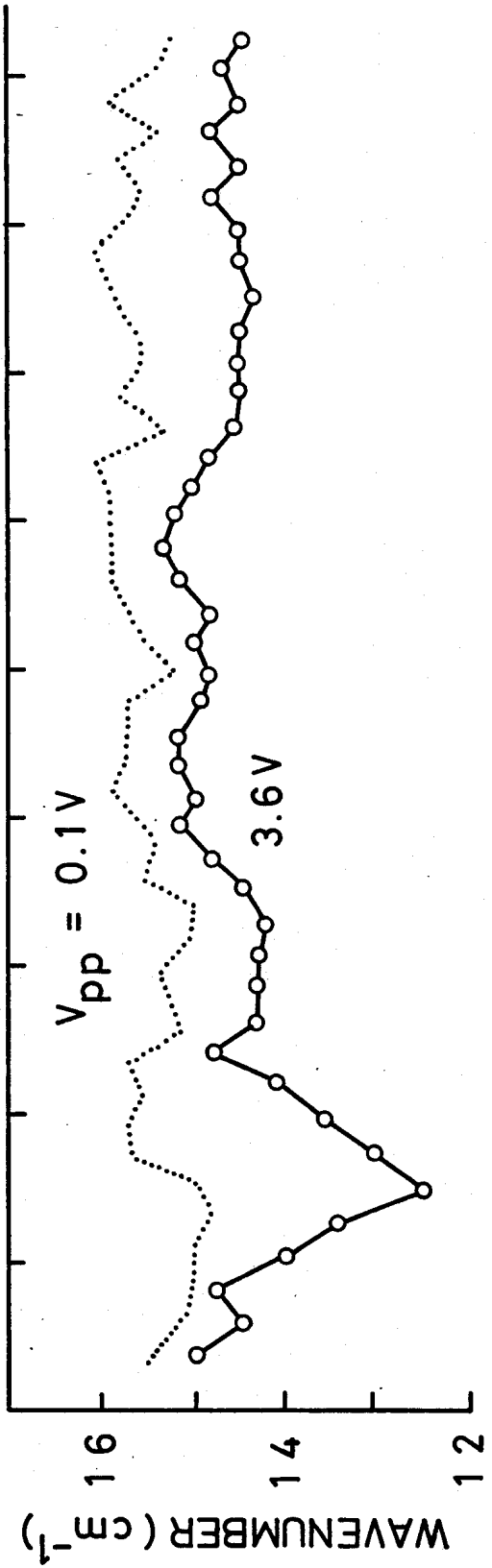
1. V.I.Karpman and E.M.Krushkal', Zh. Eksp. Teor. Fiz. 55, 530 (1968) (Sov. Phys. JETP 28, 277 (1969)); Y.H.Ichikawa and T.Taniuti, J. Phys. Soc. Japan 34, 513 (1973); V.I.Karpman, *Non-Linear Waves in Dispersive Media* (Pergamon Press, Oxford, 1975); A.Hasegawa, *Plasma Instabilities and Nonlinear Effects* (Springer-Verlag, Berlin Heidelberg New York, 1975) etc.
2. T.Kakutani and N.Sugimoto, Phys. Fluids 17, 1917 (1974).
3. V.S.Chan and S.R.Seshadri, Phys. Fluids 18, 1294 (1975).
4. H.Ikezi, K.Schwarzenegger, A.L.Simons, Y.Ohsawa and T.Kami-mura, Phys. Fluids 21, 239 (1978).
5. S.Watanabe, J. Plasma Phys. 17, 487 (1977).
6. R.J.Taylor, K.R.McKenzie and H.Ikezi, Rev. Sci. Instrum. 43, 1675 (1972); R.Limpaecher and K.R.McKenzie, Rev. Sci. Instrum. 44, 726 (1973).
7. K.J.Harker and D.B.Illic, Rev. Sci. Instrum. 45, 1315 (1974).
8. H.W.Hendel, M.Yamada, S.W.Seiler and H.Ikezi, Phys. Rev. Lett. 36, 319 (1976); B.D.Fried and A.Y.Wong, Phys. Fluids 9, 1084 (1966).
9. T.Taniuti and N.Yajima, J. Math. Phys. 10, 1369 (1969).
10. R.Z.Sagdeev, *Reviews of Plasma Physics* (Consultants Bureau, New York, 1966) Vol.IV.

Figure Captions

- Fig.1. Dispersion relation of linear waves in an ion beam-plasma system with beam velocity $v_b \sim C_s$. Here, computation is made for $v_b = 1.1 C_s$, density ratio $N_b/N_e = 0.15$, temperature ratios $T_e/T_i = 5$ and $T_e/T_b = 15$. F: fast ion beam mode, S: slow ion beam mode, A: ion acoustic mode. Dispersive phase velocity v_p and group velocity v_g computed for the same condition are also given.
- Fig.2. Raw data of the nonlinear wavenumber shift and amplitude of a large amplitude carrier wave as function of distance.
- Fig.3. Carrier wave signals evolving with distance x . These are obtained at $\omega_o/2\pi \approx 587$ kHz and $v_b \approx 1.4 C_s$. Here, the applied rf voltage (top trace) is externally modulated at 620 Hz.
- Fig.4. (a) Frequency spectra of signals received by a probe at various rf voltage V_{pp} . (b) Frequency spectra of received signals evolving with distance x .
- Fig.5. Initial carrier (Δ), low frequency (O) and lower sideband (\bullet) wave amplitudes as function of the rf voltage V_{pp} .
- Fig.6. Amplitudes of the carrier (Δ), low frequency (O) and lower sideband (\bullet) waves changing with distance x .
- Fig.7. Typical carrier wave envelope splitting into a train of wave packets.
- Fig.8. (a) Schema of wave packet. (b) Histograms for the local carrier frequencies on the upstream and downstream sides. Here, ω_{av} is the frequency averaged over the wave packet.
- Fig.9. Model of evolving wave packet.

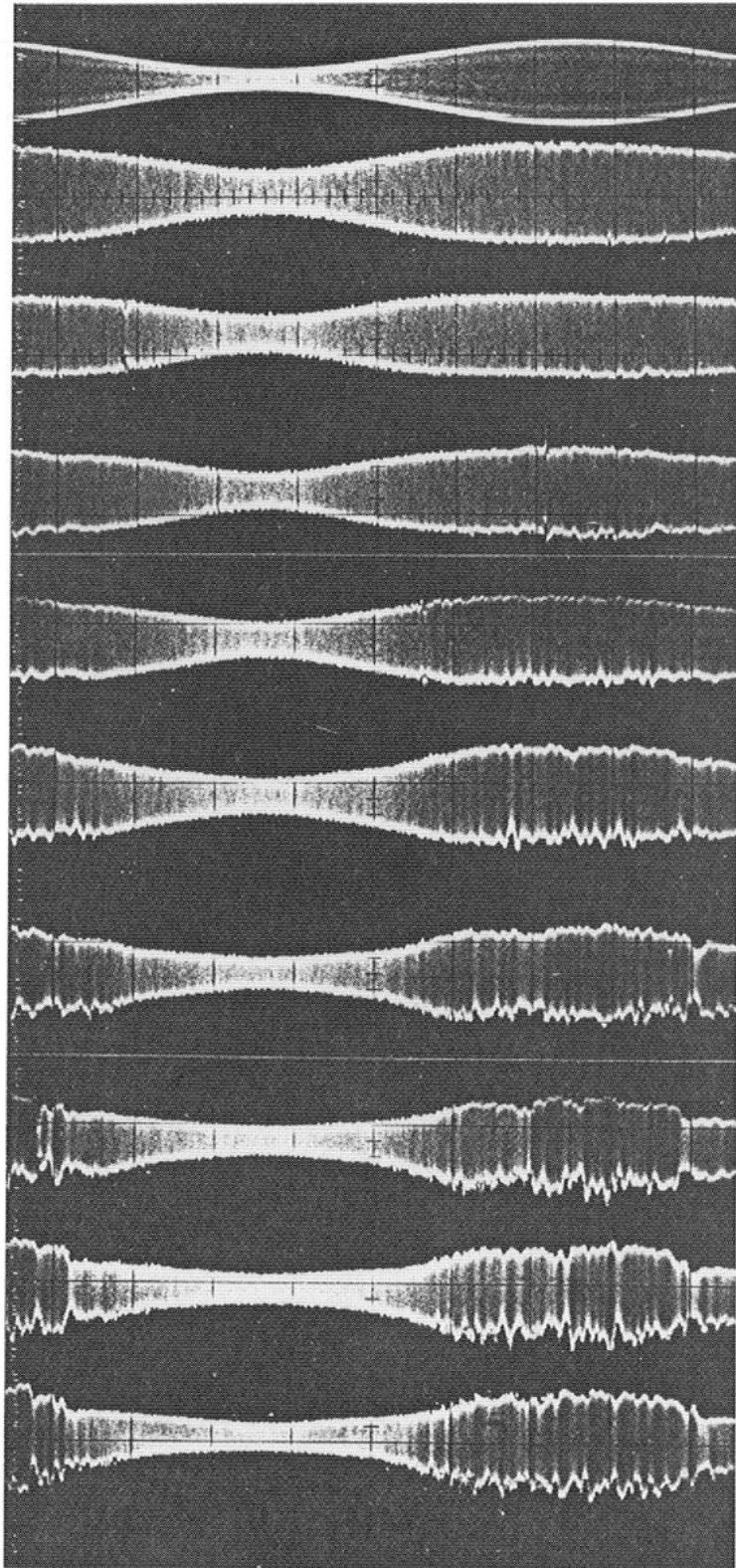


[Fig. 1]



[Fig. 2]

$$\omega_0 / 2\pi = 587 \text{ kHz}$$



applied RF
voltage

signal at
 $X = 0.4 \text{ cm}$

0.8

1.3

1.8

2.3

2.8

3.3

3.8

4.4



$200 \mu\text{s}/\text{div}$

[Fig. 3]

$$\omega_0 / 2\pi = 663 \text{ kHz}$$

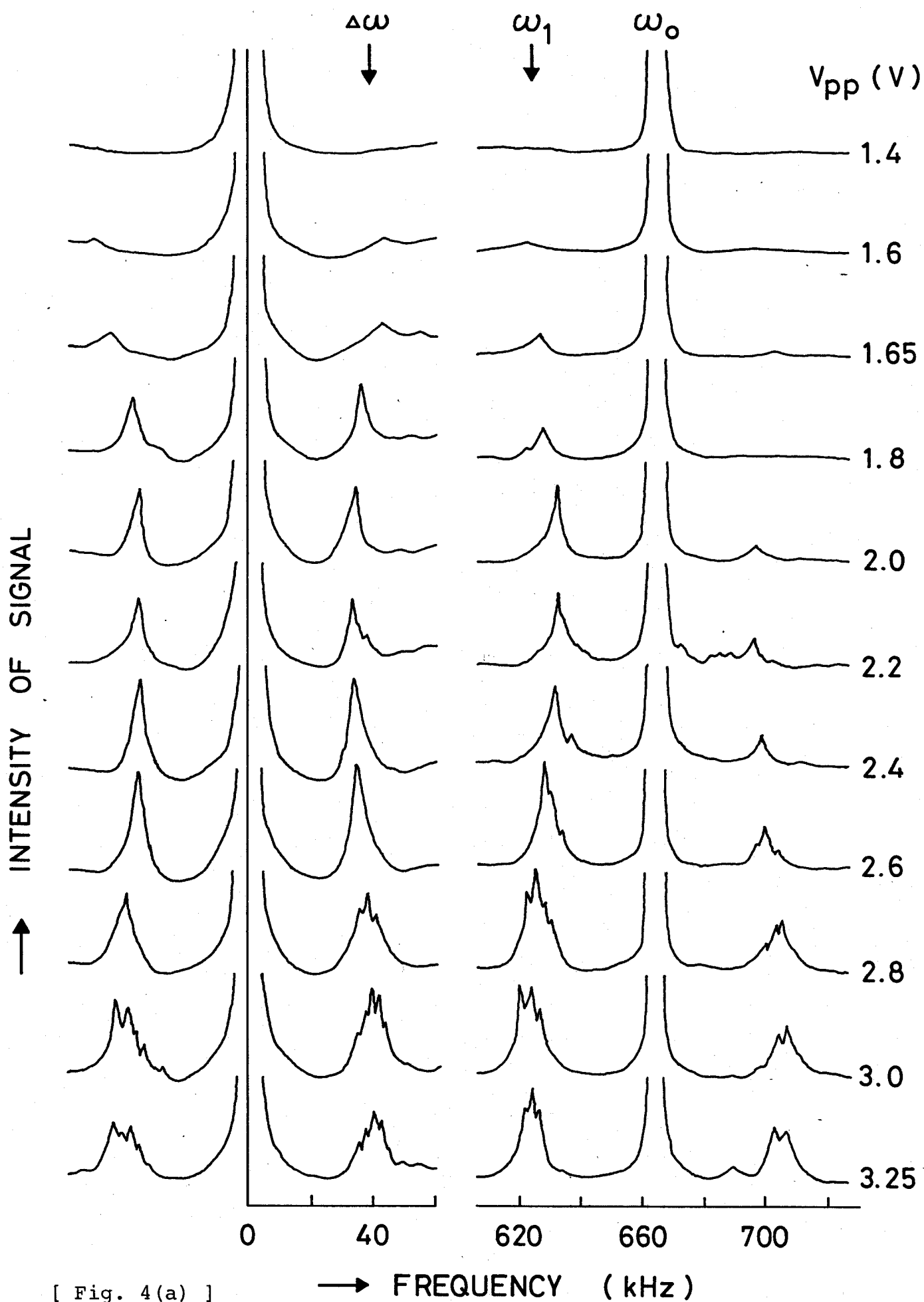


[Fig. 4(a)]

$$\omega_0/2\pi = 644 \text{ kHz}$$

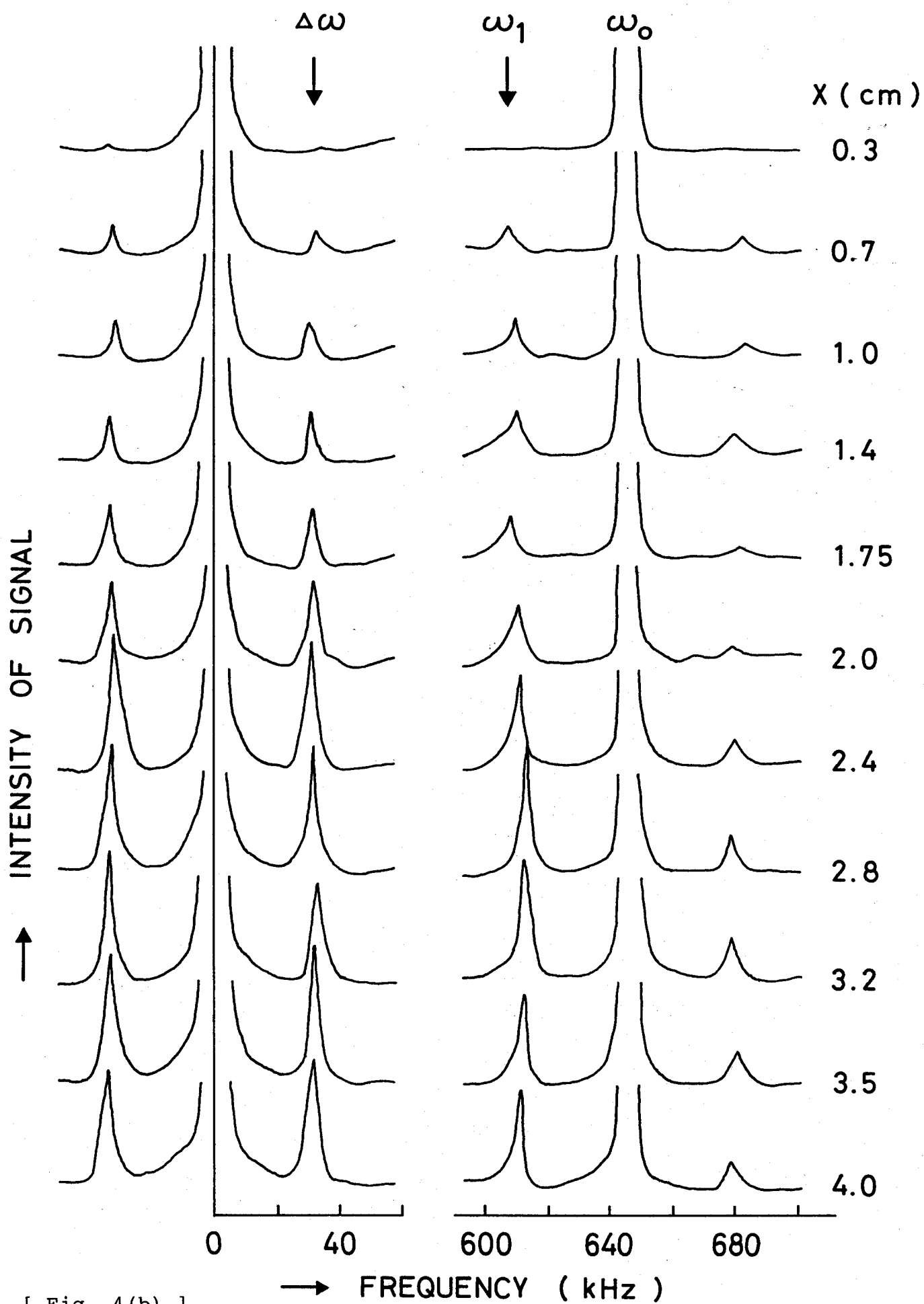


[Fig. 4(b)]

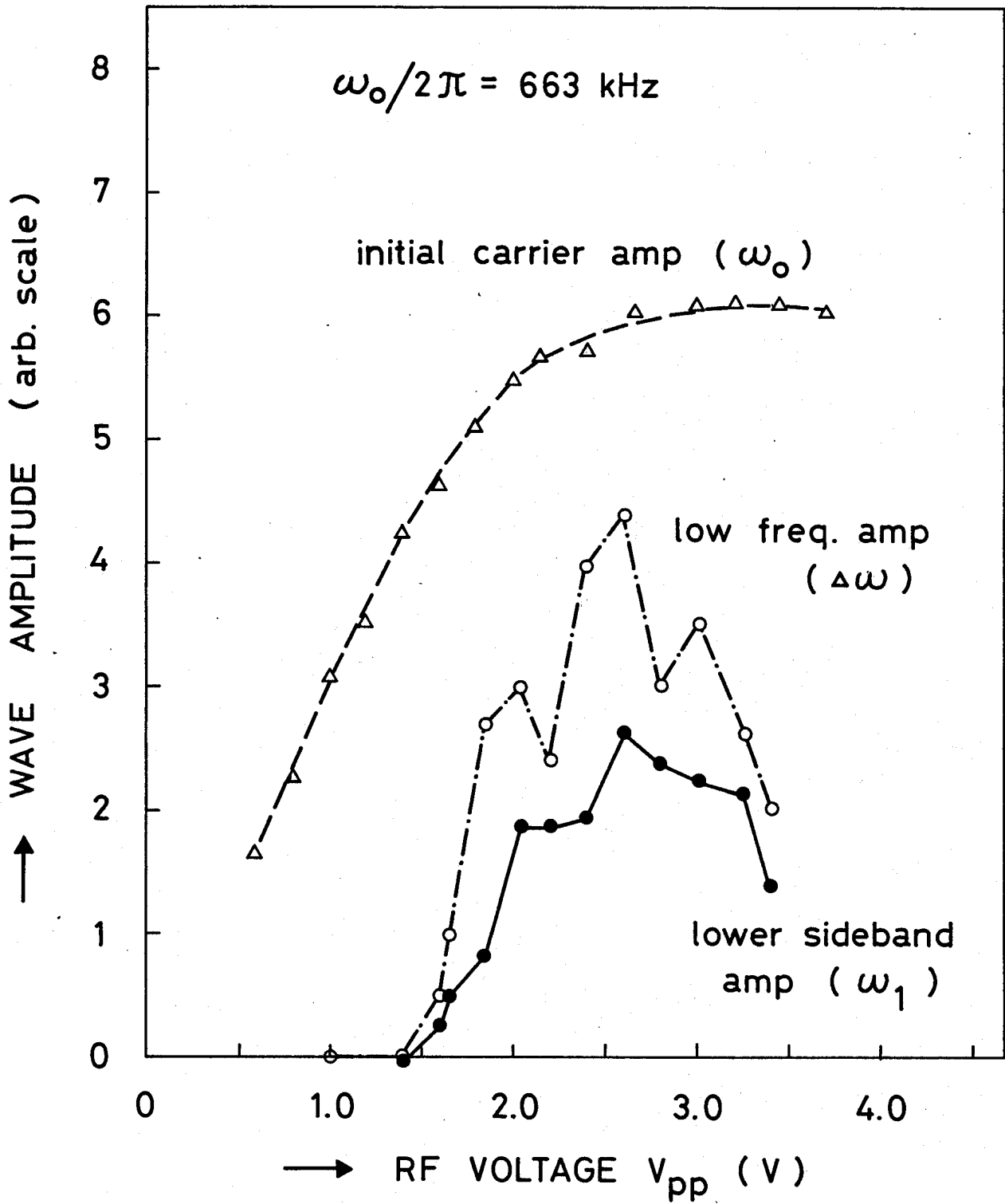


[Fig. 5]

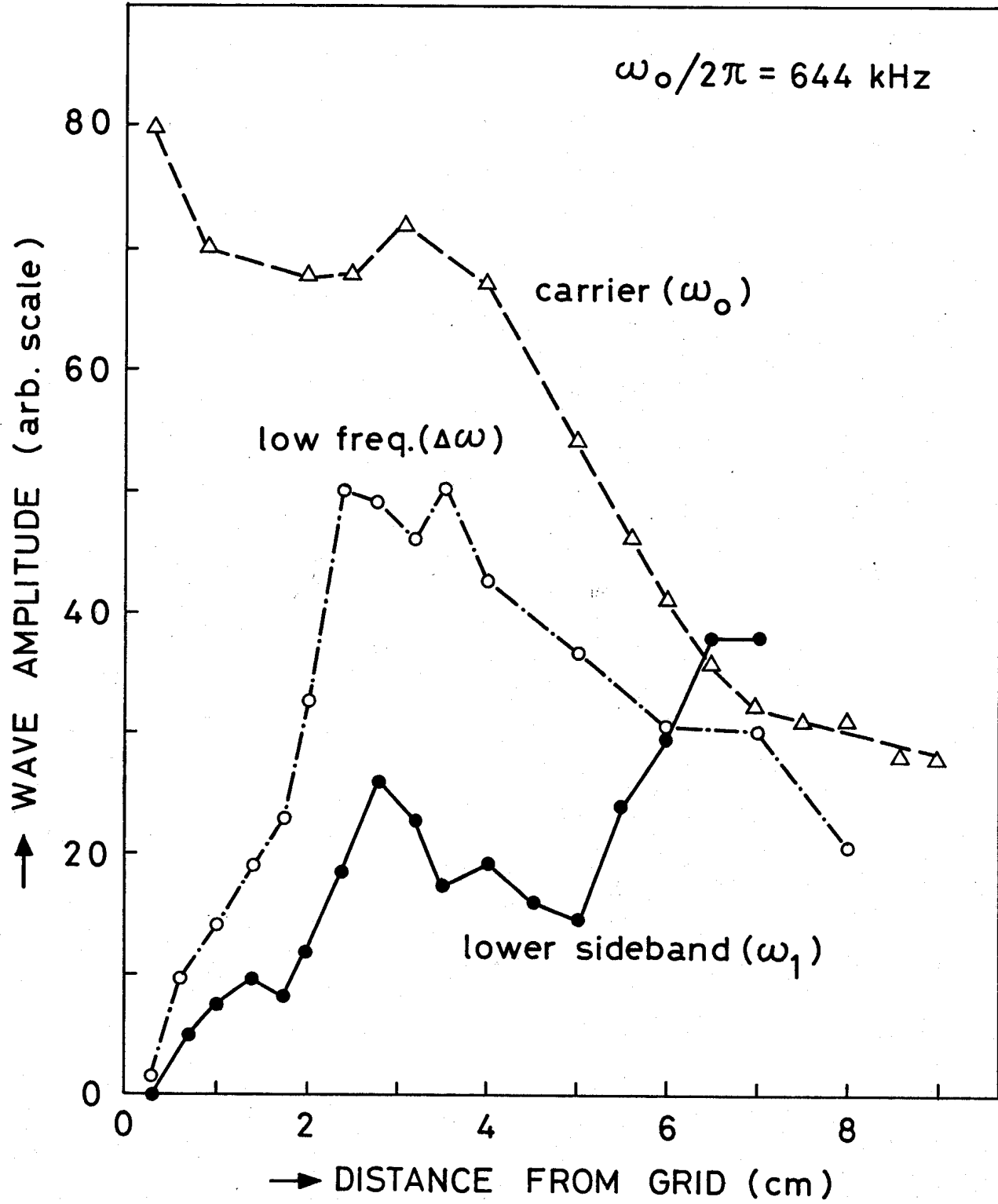
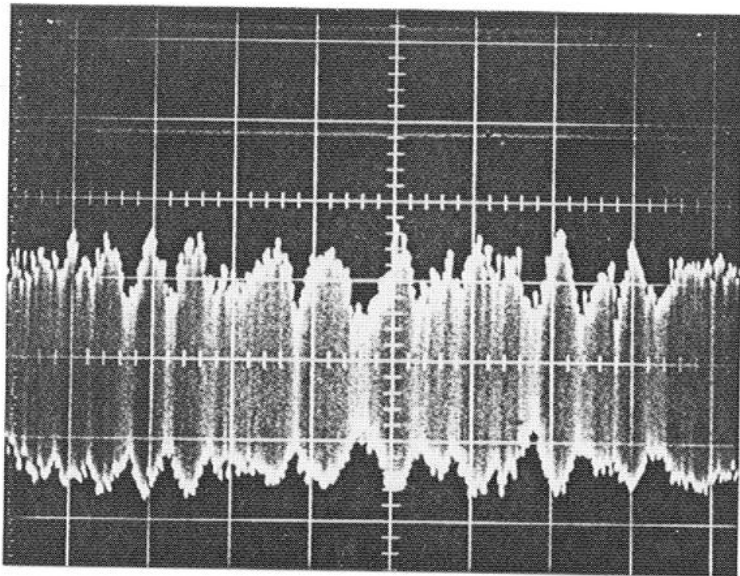


[Fig. 6]

$$\omega_0/2\pi = 649 \text{ kHz}$$



→ | ←
50 μ s/div

[Fig. 7]

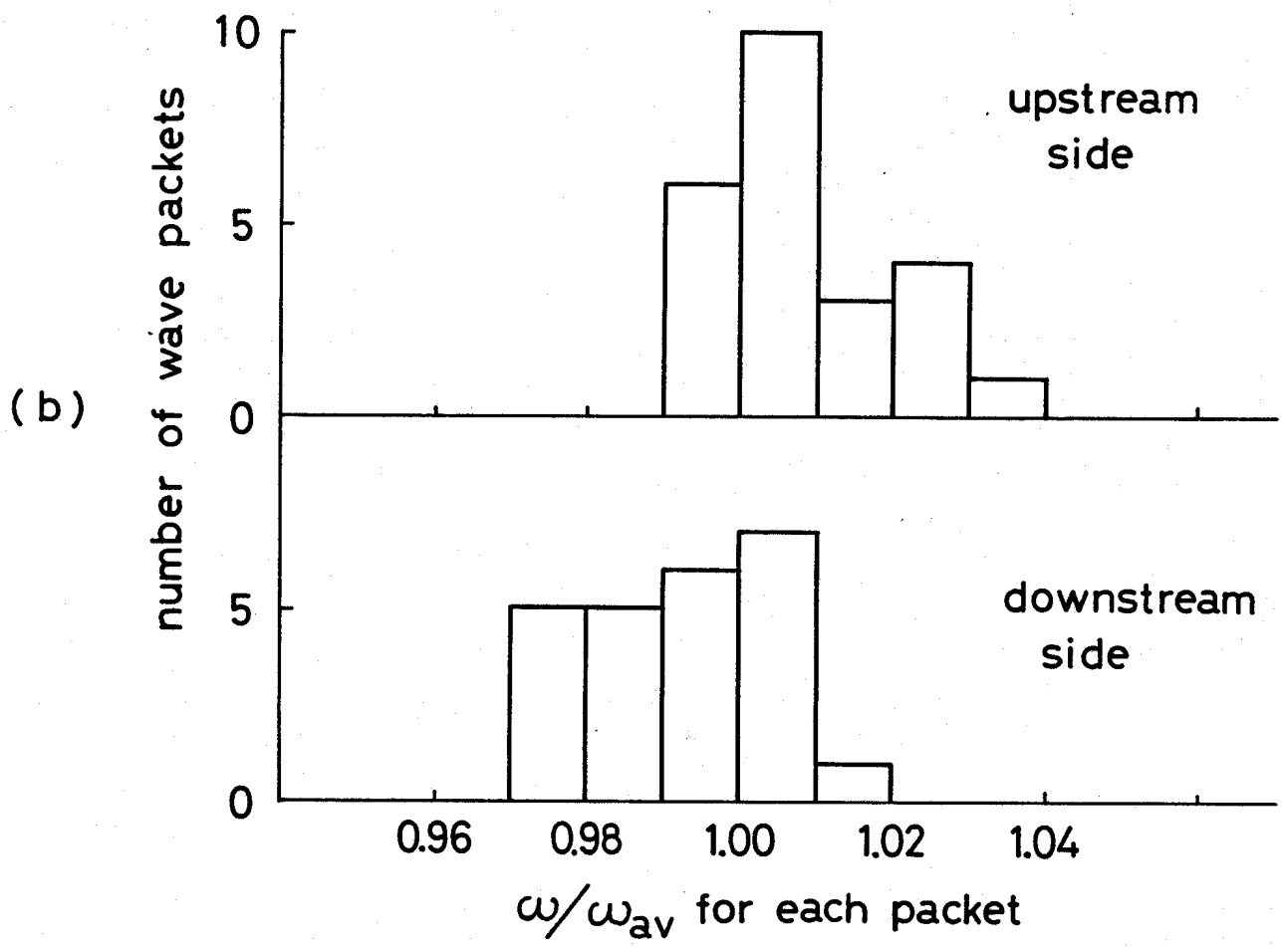
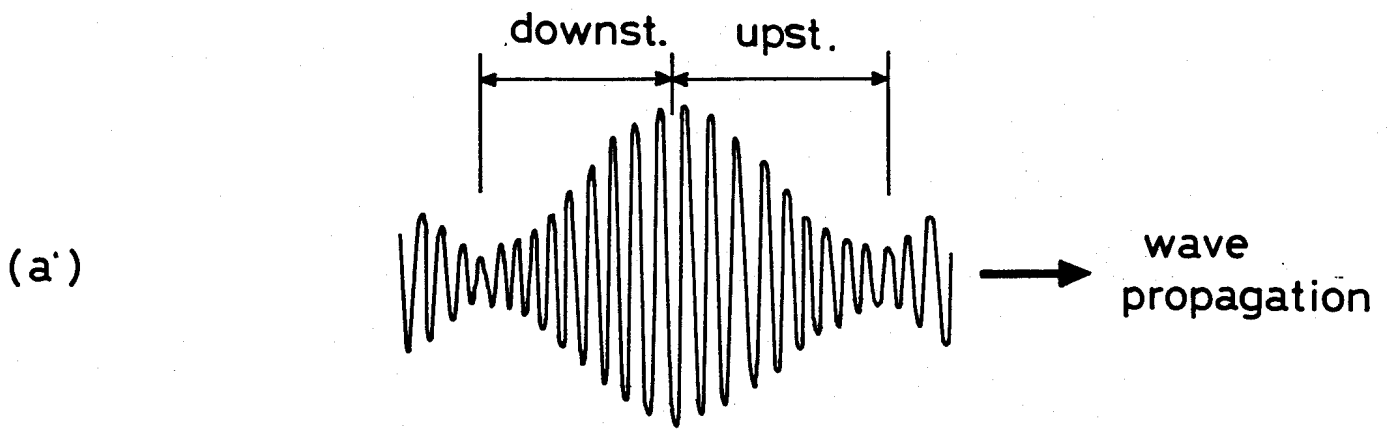


[Fig. 8]

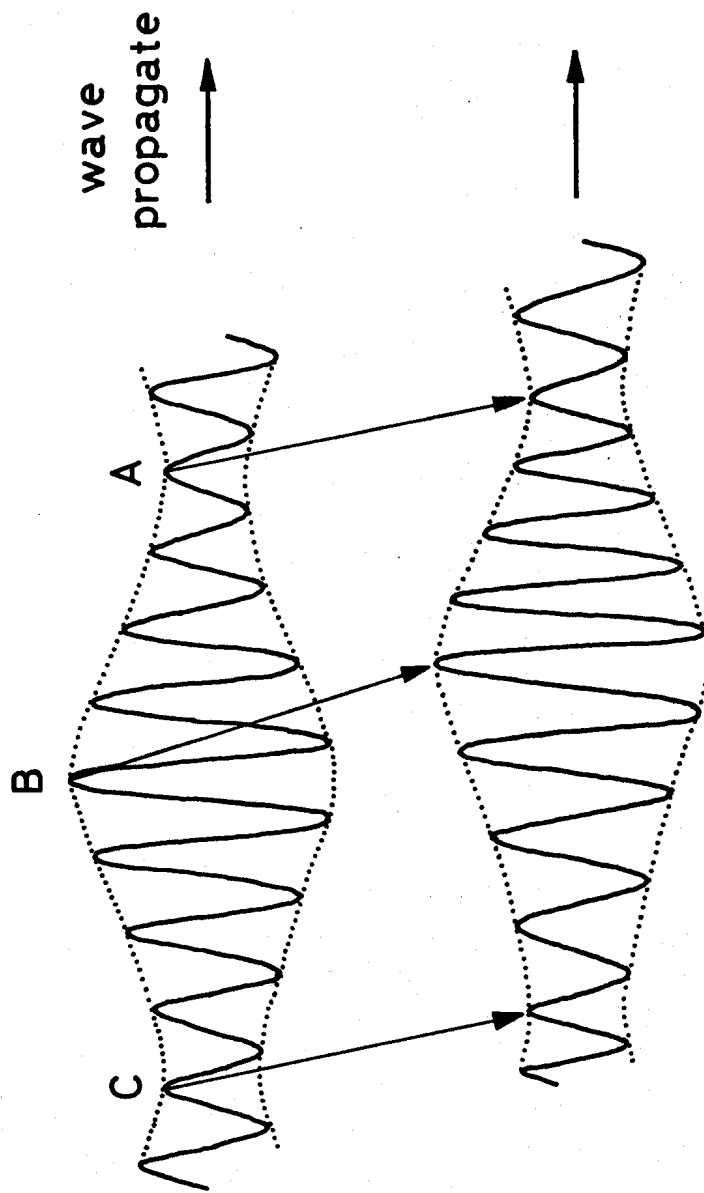


[Fig. 9]